Carbon nanotube caps as springs: Molecular dynamics simulations

Nan Yao* and Vincenzo Lordi
Princeton Materials Institute, Princeton University, Princeton, New Jersey, 08540
(Received 13 July 1998)

We present a detailed investigation of the spring behavior of carbon nanotube caps. We show that the caps act as harmonic springs, responding linearly to axial forces for appreciable displacements. Interestingly, we find the spring constant to be essentially independent of diameter and number of layers, but the maximum harmonic displacement increases with tube diameter and especially with number of layers. This spring effect is significant when the tubes are sufficiently short so that buckling does not occur before cap compression. [S0163-1829(98)05340-5]

Carbon nanotubes exhibit mechanical properties that are remarkably different from other known materials and are expected to have a great potential for many nanoapplications.[1–5] Work is currently underway studying the use of nanotubes as minuscule field-emission electron guns,[6,7] tiny test tubes,[8] and tips for atomic force microscopy[9] (AFM). Ultratough composite materials using nanotube ''fibers'' can also be imagined. The mechanical properties of nanotubes are important since the design of any potential application depends on these properties. Nanotube bending, twisting, buckling, and curvature effects were studied.[1,5,10–12] Young's modulus was estimated experimentally using transmission electron microscopy, giving an exceptionally high average value of $Y=1.8$ TPa.[4] Recently, we have shown using molecular dynamics (MD) simulations that nanotubes are of such small dimension that variations in tube geometry can affect the Young's modulus.[13] In another paper, we examined the elastic response of nanotubes to asymmetrical radial compressive forces.[14] In this paper, we report in detail the dynamics of a nanotube under axial stress, for example, if a nanotube were used for AFM. We find that for suitably sized tubes, the tips act as Hookean springs for appreciable displacements.

MD simulations were performed with Cerius[2] by Molecular Simulations, Inc., using the universal force field (UFF) developed by Rappé *et al.*[15] Force-field based simulations are convenient since they use an explicit expression for the potential energy surface of a molecule as a function of the atomic coordinates. UFF is a purely harmonic force field with a potential energy expression of the form:

$$E=E_R+E_\theta+E_\phi+E_\omega+E_{vdW}+E_{\mathrm{el}}. \tag{1}$$

Bond stretching E_R is described by a harmonic term. Bond angle bending E_θ is described by a three-term Fourier cosine expansion. Torsions E_ϕ and inversions E_ω are described by cosine-Fourier expansion terms. van der Waals interactions E_{vdW} are described by a Lennard-Jones potential. Electrostatic interactions E_{el} are described by a Coulombic term. The functional form of each energy term is given in Eq. (2),

$$E_R=k(r-r_0)^2,$$

$$E_\theta=k(C_0+C_1\cos\theta+C_2\cos 2\theta),$$

with

$$C_2=1/(4\sin^2\theta_0),$$

$$C_1=-4C_2\cos\theta_0,$$

$$C_0=C_2(2\cos^2\theta_0+1),$$

$$E_\phi=k(1\pm\cos n\phi), \tag{2}$$

$$E_\omega=k[1+\cos(n\chi-\chi_0)],$$

$$E_{vdW}=\varepsilon\left[\left(\frac{r^*}{r}\right)^{12}-2\left(\frac{r^*}{r}\right)^{6}\right],$$

$$E_{\mathrm{el}}=\frac{q_iq_j}{\varepsilon r_{ij}}.$$

Additionally, a Wilson, or umbrella, out-of-plane term of the form $k(\cos\chi-\cos\chi_0)^2$ may be included. Definitions of the variables in Eq. (2) can be found in Ref. 15, along with a more complete discussion of the particular forms of the potential functions. For nanotubes, the carbon atoms have not net charge, so the E_{el} term is always zero.

Parameters were determined for a wide range of molecules and cover the entire Periodic Table. Initial tests indicated that UFF quantitatively describes aromatic organics fairly well.[15] Our own MD tests of simple graphite systems using UFF were qualitatively accurate in behavior and quantitatively accurate in layer spacing, bond lengths, and bond angles.[16]

For our study, we modeled various symmetrically capped nanotubes with armchair helicity, composed of one or more (n,n) concentric shells. Layers of the multiwalled tubes were constrained at the open end to not slide within each other, simulating real tubes, which ordinarily do not have such freedom. The cap of the smallest tube used in our simulations (10,10) is the hemisphere obtained by cutting C_{240} in half. The other tubes have caps with identical morphology, but pentagons spaced farther apart. The smallest tube we studied involved 1890 atoms.

Two sets of MD simulations were performed: in one experiment, a C_{60} molecule was ''fired'' at the tip of the tube, along the direction of the tube axis, at 22 Å/ps, (2200 m/s)

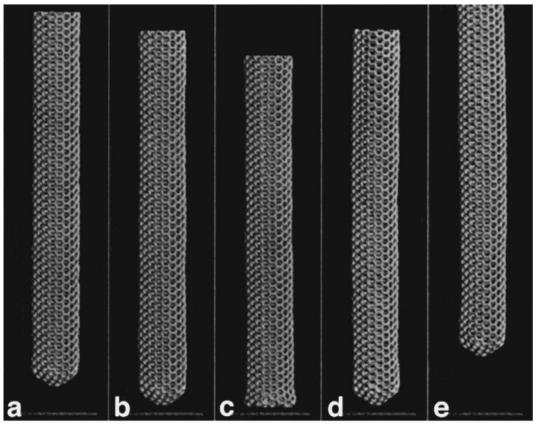

FIG. 1. Frames from MD simulations of a capped (10,10) nanotube pushed onto a fixed graphite surface at $t=$(a) 0.00, (b) 0.60, (c) 1.55, (d) 2.50, and (e) 4.00 ps.

while the opposite end of the tube was held fixed; in the other experiment, the tube was pushed into a fixed sheet of graphite at 10 Å/ps (1000 m/s) with the tube axis perpendicular to the graphite plane. (See Fig. 1.) While the velocities involved in these simulations are probably exceptionally high, they result in collision forces on the same order of magnitude (ones to tens of nN) as is typical in AFM.[9]

Both simulations showed qualitatively the same behavior. Upon collision, the symmetrical cap compresses into the hollow of the tube, acting as a ''shock absorber.'' Figure 1 shows a few frames from a collision simulation and the shape of the tip at various times during the collision. A schematic of the cap deformation is given in Fig. 2. It is evident that large bond angle strains must be incurred for such drastic tip deformation; however, the necessary forces are not very large. In the above simulations, the force exerted on the tip of the tube is less than 10 nN. Each atom at the tip feels only a few nN of force.

The spring behavior of the caps was calculated by tracking the potential energy of the tubes during compression. The results for the (10,10) tube are shown in Fig. 3, which is a plot of the relative potential energy of the tube as a function of tip displacement. A harmonic (Hookean) region is clearly visible for displacements of less than ~1.6 Å for this tube. For greater displacements, the potential energy appears to vary linearly with displacement. The data up to 1.6 Å were fit to a quadratic function of the form kx^2 to obtain the spring constant k. For a Hookean spring $U=kx^2/2$. The thick dashed line in Fig. 3 indicates the magnitude of the restoring

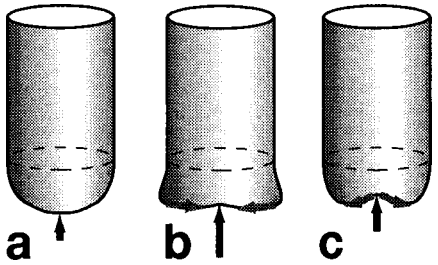

FIG. 2. Schematic of tip compression process (a) initially, (b) at critical point, and (c) after critical point. (Scale is not proportional to actual tube sizes.)

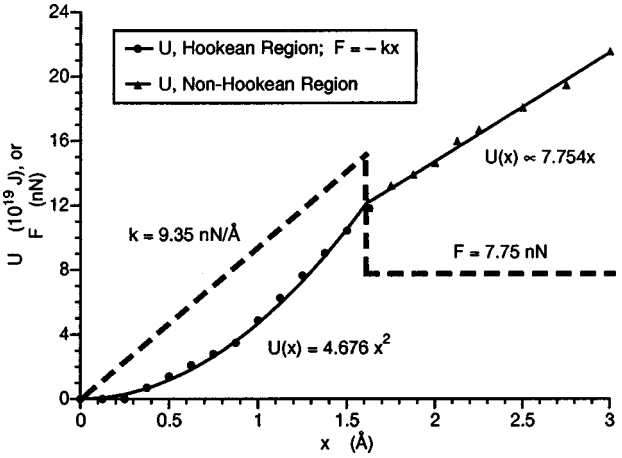

FIG. 3. Plot of potential energy U vs displacement x for the (10,10) tube pictured in Fig. 1. The thick dashed line is the restoring force $F=-\partial U/\partial x$, 1.60×10^{-19} J=1 eV.

force produced by a given displacement, found from $F=-\partial U/\partial x$. It is interesting to note that a discontinuity exists and that beyond the region where Hooke's law is obeyed, a smaller force is required to further compress the tip up to a certain distance. This arises because when the tip is first compressed, the applied force works to distort the shape of the cap, essentially pushing the cap's walls outward as shown in Figs. 2(a) and 2(b). After the maximum (critical) strain is reached [Fig. 2(b)], any further force works against the ''springs'' of the bonds at the perimeter of the cap that are trying to push the tip back ''down,'' illustrated in Fig. 2(c). Bonds are no longer very strained, but instead are creating a constant ''drag'' on the tip.

Simulations on other symmetrically capped tubes of various diameter and number of layers produced similar results, which are summarized in Table I. The spring constant is about the same for all the tubes, averaging ~9.8 nN/Å, which is related to the strength of the C-C bonds in nanotubes. The maximum (critical) displacement for harmonic response, however, increases for larger diameter tubes. Interestingly, for tubes with more layers but identical outer diameter a large increase in the maximum harmonic displacement is seen, since interlayer interactions prevent critical distortion from being reached until greater displacement. The inner layers create extra resistance for the external force, which must distort all of the layers.

The elastic response of asymmetrical tips is more difficult to characterize since the compression is very dependent on tip geometry, which can vary from tube to tube, and also can involve the tube walls. Asymmetrical tips would not be desirable for applications such as AFM, and are not considered here, since the tip compression is complex and difficult to predict.

While the forces involved in the cap compressions are on the order of tens of nN or less, their magnitudes must be put into perspective. When a nanotube is crashed into a surface, we could imagine a force resulting in buckling of the tube, thus preventing significant local compression of the tip. As described by Euler in the 1700s, a tube or rod in axial compression will remain straight until a critical force is reached when bifurcation occurs. This critical buckling force is given by[9] $F_{\mathrm{Euler}}=\pi^2 YI/L^2$, where Y is the Young's modulus, L is

TABLE I. Elastic constant and critical buckling force for various nanotubes short enough to allow cap compression before buckling. N=number of layers; a, b=outer, inner radii, respectively, in Å; L, length, in Å; Y, Young's modulus, in TPa; F_{Euler}, buckling force, in nN; k, elastic constant, in nN/Å; x_{elastic}, maximum elastic compression, in Å. Y data are taken from Ref. 13.

	Tube	N	a	b	L	Y	F_{Euler}	k	x_{elastic}
1	(5,5)	1	5.1	1.7	96.4	1.12	6.25		
2	(10,10)	1	8.5	5.1	96.8	1.02	38.34	9.35	1.6
3	(15,15)	1	11.9	8.5	96.5	1.00	123.5	9.10	1.7
4	(20,20)	1	15.3	11.9	96.5	0.97	280.5	10.5	1.8
5	(10,10)/(15,15)	2	11.9	5.1	96.5	1.01	162.9	10.6	2.2
6	(10,10)/(15,15)/(20,20)	3	15.3	5.1	96.5	1.03	464.0	9.14	4.0

the length, and I is the area moment of inertia of the beam, given by[2] $I=\int_A z^2 dA$. For a tube of annular cross section $I=\pi(a^4-b^4)/4$, with a and b specifying the outer and inner radius, respectively. Then, the critical buckling force of a nanotube is calculated from Eq. (3):

$$F_{\text{Euler}}=\pi^3 Y(a^4-b^4)/4L^2. \tag{3}$$

Table I lists values of F_{Euler} for uncapped tubes of various radii and length. The tubes are uncapped to allow accurate calculations since Eq. (3) assumes a constant annular cross section. Thus, the table lists a minimum value for the buckling force of a capped nanotube since the cap's shape allows some, but not all, of the applied force to be transferred to the walls of the tube. The values for Y listed in Table I and used in Eq. (3) were derived from MD simulations described in our previous report.[13]

We can see from Eq. (3) and Table I that F_{Euler} becomes very sensitive to the tube dimensions as the size of the tube gets smaller. For tubes of the size used in our simulations (tubes 2–6), the critical buckling force is much greater than the force require to push in the tube's tip. However, for a tube of the same diameter, but ten times longer, the buckling force is so small that significant compression of the tip would not occur. Therefore, such compression of a capped nanotube tip as described above is a realistic phenomenon, provided the tube is of appropriate dimensions (i.e., short enough or of great enough diameter). Essentially, the tube length determines the appearance of this effect, since nanoapplications ordinarily require the smallest diameter tubes possible.

We show with this study that the tip of a symmetrically capped nanotube can act as the world's smallest Hookean spring when compressed axially. This behavior is significant when the tube is sufficiently short that buckling does not occur before cap compression, and persists for an appreciable range of displacements, depending on the diameter of the tube and the number of layers, with a spring constant of ~9.8 nN/Å essentially independent of tube size. Constructing an AFM tip from a thin nanotube short enough to undergo tip compression from an axial force may allow an advancement in atomic probe technology utilizing the Hookean spring nature of the cap, which behaves as though attached to the end of a rigid rod. Such next generation AFM tips also would provide much higher spatial resolution than current tips due to their tiny diameter. We believe, additionally, that this study demonstrates the importance of atomic level calculations (e.g., though MD simulations) for accurate predictions of nanotube dynamics, owing to the extremely small size scale. At the nanoscale, significant atomic effects are not properly accounted for by continuum calculations.

We wish to thank M. M. J. Treacy and T. W. Ebbesen for valuable discussions. This work was supported by the Materials Research and Engineering Center program of the National Science Foundation (Grant No. DMR-94-00362).

*Electronic address: nyao@princeton.edu

[1] B. I. Yakobson, C. J. Brabec, and J. Bernholc, Phys. Rev. Lett. **76**, 2511 (1996); B. I. Yakobson and R. Smalley, Am. Sci. **85** (7/8), 324 (1997).

[2] G. Overney, W. Zhong, and D. Tománek, Z. Phys. D **27**, 93 (1993).

[3] J. Tersoff and R. S. Ruoff, Phys. Rev. Lett. **73**, 676 (1994); R. S. Ruoff *et al.* Nature (London) **364**, 524 (1993).

[4] M. M. J. Treacy, T. W. Ebbesen, and J. M. Gibson, Nature (London) **381**, 678 (1996).

[5] s. Iijima *et al.*, J. Chem. Phys. **104**, 2089 (1996); J. F. Despres, E. Daguerre, and K. Lafdi, Carbon **33**, 87 (1995).

[6] A. G. Rinzler *et al.*, Science **269**, 1550 (1995).

[7] W. A. De Heer, A. Châtelain, and D. Ugarte, Science **270**, 1179 (1995).

[8] D. Ugarte, A. Châtelain, and W. A. de Heer, Science **274**, 1897 (1996).

[9] H. Dai *et al.*, Nature (London) **384**, 147 (1996).

[10] O. Stéphan, P. M. Ajayan, C. Colliex, F. Cyrot-Lackmann, and É. Sandré, Phys. Rev. B **53**, 13 824 (1996).

[11] D. H. Robertson, D. W. Brenner, and J. W. Mintmire, Phys. Rev. B **45**, 12 592 (1992).

[12] M. R. Falvo *et al.* Nature (London) **389**, 582 (1997).

[13] N. Yao and V. Lordi, J. Appl. Phys. **84**, 1939 (1998).

[14] V. Lordi and N. Yao, J. Chem. Phys. **109**, 2509 (1998).

[15] A. K. Rappé *et al.*, J. Am. Chem. Soc. **114**, 10 024 (1992); C. S. Casewit, K. S. Colwell, and A. K. Rappé, *ibid.* **114**, 10 035 (1992); A. K. Rappé, K. S. Colwell, and C. J. Casewit, Inorg. Chem. **32**, 3438 (1993).

[16] V. Lordi and N. Yao (unpublished).